



Conceptual Design of a Low Noise Hybrid Passenger Aircraft

Jason **Bonni**, Bianca **Burghoff**, Eray **Dinçer**, Jonas Felix Lambert **Eichler**, Thomas **Ferguson**, Humza **Mirza**, Miguel **Nuño**, Miguel Yael **Pereda***, Martin **Valley**

Institute of Aeronautics and Astronautics, Wüllnerstraße 7, 52062 Aachen, RWTH Aachen University
(Dated: July 1, 2017)

The European Flight path 2050 along with NASA Environmentally Responsible Aviation N+ Series have set targets for reductions in noise and gas emissions. Here we present a conceptual aircraft with hybrid propulsion system using the airframe design to shield noise and achieve ultra-low emission levels. We found that a narrow body aircraft in a canard and a high wing configuration equipped with a turbine powering quad electrical fans via batteries located on top of the main wing as the most promising design. Our design demonstrates that the sound propagation from the turbine and electrical fans can be shielded using the airframe. By integrating the shortened landing gears inside the vertical stabilizers beneath the main wing allowed weight reductions. Potentially, the designed aircraft offers noticeable noise reductions and environment conservation. We anticipate our design to be relevant for future work and an excellent starting point for more sophisticated conceptual aircraft design.

All authors contributed equally.

* Scientific Advisor, Miguel.Pereda@ILR.RWTH-Aachen.de; <http://www.ilr.rwth-aachen.de/>

CONTENTS

I. Introduction	3
II. Configuration Details	4
II.1. Hybrid Propulsion System	4
II.2. Vertical Stabilizers with Landing Gears	5
II.3. Canard and Wing Configuration	6
III. <i>AquisPlane</i> 3D Presentation with Design Feature Highlights	7
IV. Aircraft Design	8
IV.1. Initial Sizing	8
IV.2. Engine Design	9
IV.3. MTOW Estimation	9
IV.4. Fuselage Configuration	11
IV.5. Wing and Empennage Design	11
IV.6. Control Surfaces and High Lift Devices	12
IV.7. Landing Gear Design	13
IV.8. Component Mass Estimation and Center of Gravity	13
IV.9. Stability and Control	16
V. Environmental	16
V.1. Jet Noise	16
V.2. Fan Noise	17
V.3. Airframe Noise	17
VI. Costs	18
VII. Conclusion	18
References	19
Acknowledgments	19
VIII. Technical Drawings	20

I. INTRODUCTION

This report was conducted by a group of interdisciplinary and international students at the Faculty of Mechanical Engineering of the RWTH Aachen University in Germany for a joint competition by the German Aerospace Center (DLR) and the National Aeronautics and Space Administration (NASA). The goal presented was to design a revolutionary quiet and low emission aircraft under the following fixed design criteria:

- Entry-into-Service 2025-2035
- New silent and fuel efficient propulsion systems integration
- NO_x emission reduction engine concepts with new combustion chambers and fuels
- Number of passengers higher than 200
- Effective flight operations

Significant progress has been made in the shape of industry wide cooperation, initiatives and action plans for designing and developing environment friendly aircrafts. Northrop Grumman Systems Cooperation has proposed a small 120-passenger aircraft designed for short 5,000 feet runways and equipped with ultra high bypass ratio propulsion system, ceramic composites, nanotechnology and memory alloys [1]. Massachusetts Institute of Technology (MIT) has presented a subsonic fixed wing 180-passenger D8 Double Bubble aircraft with two cylindrical fuselage bodies together lengthwise and turbofan jet engines mounted on the tail [2]. Cambridge University launched the Silent Aircraft Initiative and has presented an all lifting Blended Wing Body design called SAX-40, which shields the engine noise by the airframe [3] [4] [5]. Lockheed Martin developed an environmentally friendly supersonic airframe. GE Aviation, Cessna and Georgia Tech together have conceptualized a 20 passenger aircraft to reduce congestion by using point-to-point travel inhibiting smooth surfaces, turboprop engines and electricity generating fuel cells. technologies to reduce environmental impact [6]. The Boeing Company has presented five concepts under the project Subsonic Ultra Green Aircraft Research (SUGAR), most notably the SUGAR Volt with hybrid electric twin engine propulsion on top of a high aspect ratio truss-based wing [7]. NASA in cooperation with Boeing has developed a hybrid wing body X-48 concept aircraft with super conducting electric motors to drive the electric fans. The German Aerospace Center (DLR) has presented an Advanced Low Noise Aircraft (ALNA) with canard, contra-rotating open twin propellers and forward swept wings using parametric numerical tools [8]. Airbus has presented a concept aircraft with semi-embedded turbines shielded by the tail, curved fuselage, U-shaped tail with advance materials and technologies [9]. The aforementioned aircraft design projects can be summarized as following: **(i)** Cruising aircraft at about 0.7 Mach to save fuel **(ii)** Developing engines that require less power especially at takeoff **(iii)** Shorter runways to increase operating capacity and efficiency **(iv)** Smaller aircraft equipped for maximum 200 passengers flying shorter and cost efficient direct routes **(v)** Incorporating advanced emerging technologies, increasing efficiency via automation and leveraging digitization.

The main objective of the presented design study here is to establish a conceptual aircraft with integrated noise reduction and reduced emissions capability. In addition to these objectives and competition design conditions above, research and analysis into current aircraft and market trends was conducted in order to derive the Top Level Aircraft Requirements (TLARs) of the design, from here out named the *AquisPlane*. A short-range aircraft has been selected as reference. A greater relative growth within the next 20 years in domestic traffic is expected, as compared to international flights [10] [11]. The Airbus A320 is among the most widely used domestic short range aircraft, and in its different versions is a current and near future representative model with a large number of aircraft in operation and many orders over the short term. From a European perspective, in the year 2015 the A320 accumulated over three times more movements than its biggest competitor, the Boeing B737, at Heathrow airport [12]. Based on this reasoning, the A320-x can be regarded as representative with respect to an average European airport. To select the *AquisPlane*'s range the current air traffic system is analysed. The Hub-Spoke nature of the air traffic system and the predicted increase of mega aviation cities in the future leads to a prognosis of a median distance between hubs of about 2000 NM [10]. A passenger capacity of 210 has been selected taking into account the standard industry philosophy of iteratively stretching models to increase capacity after initial entry into service (A318-100, A319-100, A320-100 / -200, A321-100 / -200), and the new designs A320 NEO and A321 NEO with maximum seating capacities of 180 and 230 respectively. The cruise mach number and flight level have been reduced in comparison to the A320-200 due to the relatively low state of maturity of the selected hybrid propulsion system technology. These values have been estimated and will be discussed further. Since the airport infrastructure is not expected to drastically change within the next ten to twenty years the same Balanced Field Length (BFL) and Landing Field Length (LFL) as the A320-200 have been selected. The *AquisPlane* TLARs are summarised in Table I.

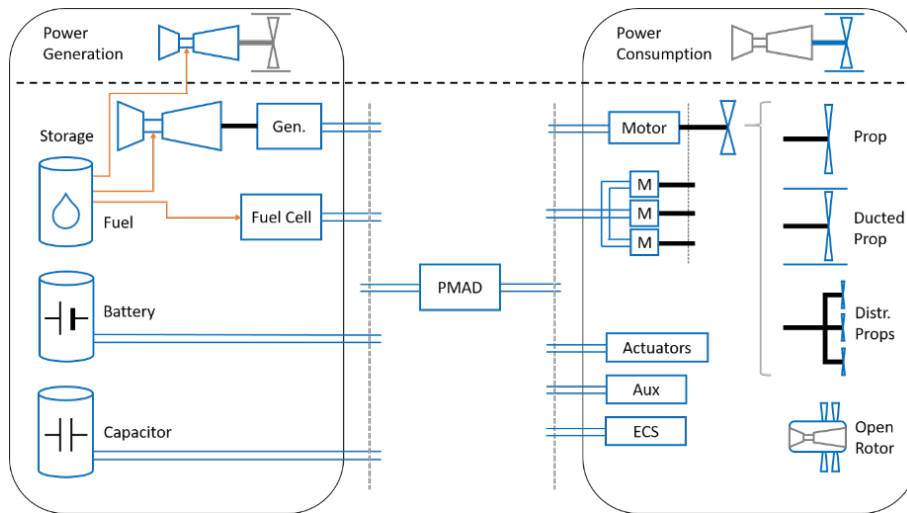
TABLE I: Top Level Aircraft Requirements of the designed aircraft

Parameter	AquisPlane A320-NEO	
Range	2000	2500
Passengers	210	150
Cruise Mach	0.65	0.78
Cruise Level	30000	35000
BFL	2300	2300
LFL	1600	1600

II. CONFIGURATION DETAILS

II.1. Hybrid Propulsion System

Conventionally civil transportation aircraft are powered by kerosene fuelled turbofan engines, which provide an overall efficiency of approximately 30% at cruise conditions [13]. Nowadays advanced aircraft propulsion concepts include electrical components or are even full electric like the Airbus E-Fan. Fig. 2 provides an overview of various existing propulsion technologies. On the left side, a variety of power sources are displayed and connected with the power consumers on the right side via the Power Management and Distribution System (PMAD), which includes all power conducting components between the source and the consumption [14].

**FIG. 1:** Different engine architecture

A fully electric propulsion system provides the possibility of zero gaseous emissions, however the central problem for fully electric large transportation aircraft remains the size and weight of the energy storage system. With approximately 0.85 kW/kg [13] and an engine consumption of 20 MW they are too heavy for the selected design and additionally do not shed weight during flight. As a result the landing weight would be significantly increased in comparison to conventional aircraft, with the consequent increase in structural weight. A stand-alone electric propulsion system in the short to mid-term does not seem feasible. Today the first Ultra High Bypass Turbofans (UHBT) are entering into service with a Bypass Ratio (BR) over 12 providing a better fuel efficiency and reduced jet noise due to a higher mass airflow and a decreasing exhaust speed. The selected *AquisPlane* propulsion system is a hybrid system combination of both concepts. A conventional kerosene powered gas turbine is connected to an electric generator, powering in turn the four electric engines which provide the required output thrust. Decoupling the energy transformation chain allows for a better selection of the working point of the different components, leading to higher efficiencies and a consequent potential physical down-scaling. One large gas turbine demonstrates a higher thermal efficiency compared to 2 or more smaller turbines for a given power output. Since our design uses electric engines instead of gas turbine engines, their emissions are replaced by those of one gas turbine alone, generating the required electric power for the engines and internal systems. This gas turbine runs constantly at its design point, generating

electric power, with extra energy stored in the on-board battery. By operating at its optimal design point the efficiency is significantly increased, reducing the generated emissions. In flight phases where the required energy is higher than that provided by the turbine, a set of on-board batteries can supply extra power to the engines. Conversely, when the power generation exceeds the demand, such as during cruise and descent, the power storage units will be charged. The battery capacity is dimensioned according to standard emergency requirements. No Auxiliary Power Unit (APU) is included in the aircraft. Aircraft systems are powered via the gas turbine and battery storage.

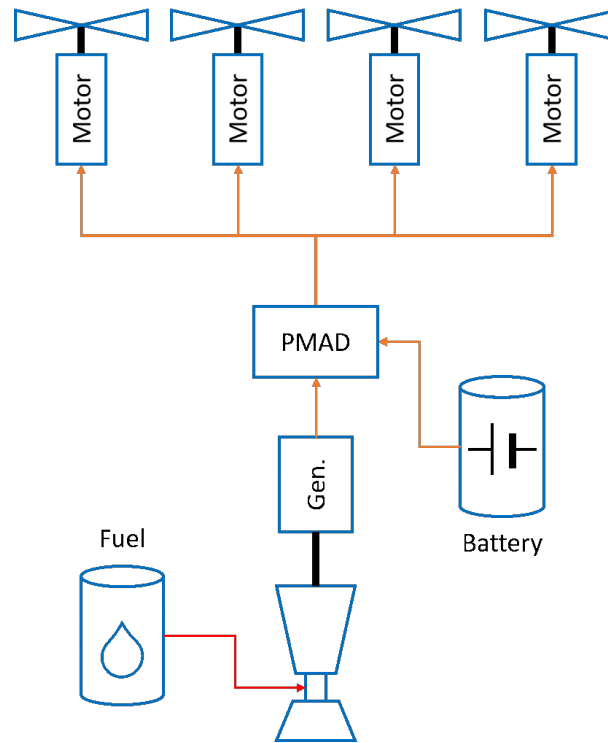


FIG. 2: The designed aircraft *AquisPlane* Propulsion System

The number and position of the electric engines have been selected according to noise criteria and the projected capabilities of this propulsion system. Due to electric engines' lack of a combustor or turbine, the only relevant remaining components of noise emission are the fan and jet noise. By positioning the engines over the wing with a certain displacement towards the wing trailing edge, an effective fan noise shielding can be expected [8]. Four engines are selected. For a given thrust and due to the logarithmic nature of the sound addition, two bigger, and hence louder, engines will produce a higher Sound Pressure Level (SPL) than four smaller, and thus quieter, engines.

The gas turbine and the mechanically coupled electric generator are positioned in the aircraft nose below the cockpit in the forward region of the cargo bay. This allows a better placement of the gas turbine inlet where free air stream conditions can be found. After the iterative design process, mass and balance criteria reinforced the decision to permit a more forward centre of gravity, increasing the moment arm allowing a lighter and smaller Vertical Stabiliser (VS). The electric energy is conducted to the batteries which are placed in the aircraft's cone-shaped tail.

II.2. Vertical Stabilizers with Landing Gears

The most revolutionary configuration decision developed in the *AquisPlane* is a twin vertical stabiliser integrated below a high wing. In the first place, a high wing is aerodynamically more efficient than a low wing [8]. This wing position also increases noise shielding for persons inside the aircraft, reducing cabin noise. To position the vertical stabilisers under the wing reduces the in-flight bending moment at the wing root. In addition, a fixed main landing gear is integrated in the vertical stabiliser. Due to the short distance to the ground, for take-off, landing and ground operations only a minimal fairing around the wheels has to be moved up, saving the weight and complexity of the hydraulic actuators and emergency extension system. This is especially advantageous since the position of the landing gear also avoids the typical interaction noise between gear vortices and wing and high lift devices of a low wing configuration [8].

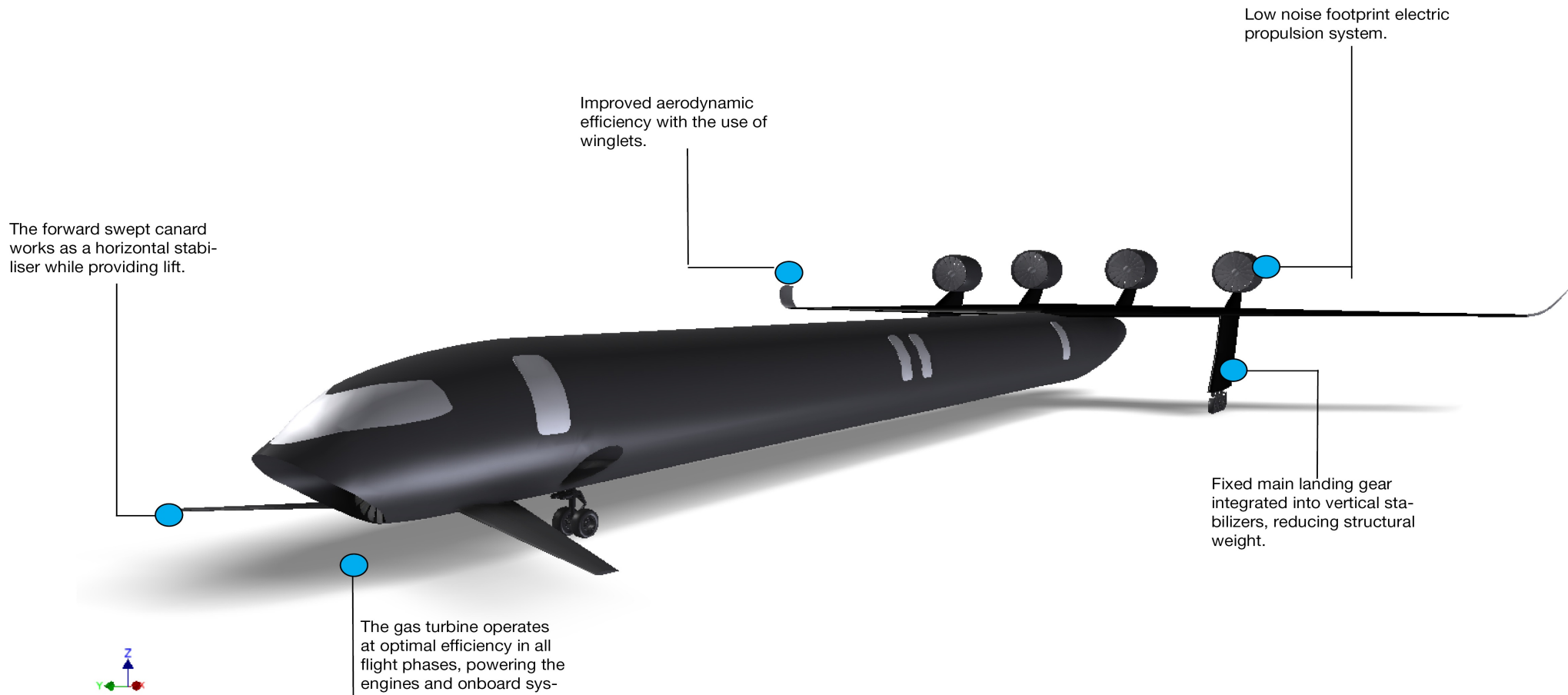
II.3. Canard and Wing Configuration

Instead of a traditional horizontal stabiliser placed at the rear of the aircraft, a canard configuration has been chosen. The idea behind this is to create a better lift distribution between main wing and canard, avoiding completely the necessity of creating negative lift irrespective of the centre of gravity position. The canard is placed in the lower part of the fuselage, increasing the vertical distance between canard and wing to reduce trailing edge wake interactions. With the wing and canard positions set, the wing design can be discussed. Sweeping a wing provides less drag at high speeds but also reduces the maximal lift coefficient of the surface. Forward-swept wings have better stall characteristics and can achieve higher lift coefficients than their backward-swept counterparts, making them more desirable from the aerodynamic point of view. This comes at the cost of a much stiffer and therefore heavier structure if classic structure construction methods are used due to divergence problems. Alternatively, taking advantage of Carbon Fiber Reinforced Polymer's (CFRP) anisotropic properties, light aeroelastically-tailored structures can also be implemented. The main wing with vertical stabilisers and engines is too complex to implement this construction method. The canard has a cleaner geometry with no heavy masses attached and can therefore be swept forward without having to expect weight penalties. For the same root position, relative to the main wing it has also the benefit of a larger moment arm, decreasing the negative interaction between the two surfaces in off-design points.

The fuel is stored in the six fuel tanks located inside the main wing and the canard. Four tanks are placed in the main wing and two tanks are placed in the canard which helps to reduce the bending moment at the root and acts as a wing vibration damper. A cross-feed valve is provided allowing the gas turbine to be fed from any of the six tanks enabling fuel trimming and assuring redundancy.

III. AQUISPLANE 3D PRESENTATION WITH DESIGN FEATURE HIGHLIGHTS

3D INTERACTIVE ILLUSTRATION - CLICK TO ROTATE IN 360°



IV. AIRCRAFT DESIGN

IV.1. Initial Sizing

Once the aircraft configuration is fixed, the initial sizing process will determine the aircraft's permitted design range, using as parameters the Wing-Loading (W/S) and Thrust-to-Weight ratio (T/W). In this manner aircraft mass, engine thrust and wing surface can be dimensioned in accordance with the TLARs and the configuration decisions.

The T/W and W/S suitable combination is made out four different flight phases: (i) take-off, (ii) climb, (iii) cruise and (iv) approach. The relations between both values are calculated using the methods from Raymer [15], Roskam [16], Jenkinson [16] and Torenbeek [17] which are resumed in Dobrev [18].

- A function of T/W to W/S can be defined based on the take-off requirements
- A maximum W/S can be calculated out of the landing distance
- The required climb power determines a minimum T/W
- The required cruise speed determines a further relationship between T/W and W/S

To find the optimal design point, the resulting curves are summarised in Fig. 4. First, however, a scaling of the graph to take-off conditions is required. This is due to the different values of thrust (altitude influence), weight (MTOW, MLW), and wing area (e.g., flap extension) in the flight phases considered. The optimum design point must be within the permitted area (shadowed area in Fig. 4). The calculations conducted here are according to EASA CS-25 specifications. For detailed information refer [19]. To select the design point, it must be taken into account that the thrust-to-weight ratio should be kept as low as possible in order to have as small and economical engines as possible, but still meet requirements. The wing loading shapes the wing surface. A larger wing loading corresponds to a relatively smaller wing. This is advantageous since a lower friction drag and a lower structural weight can be achieved. On the other hand, a better climb performance, the necessity of smaller high-lift devices and the lower induced and wave drag speak for a larger wing and thus a smaller wing loading. A compromise must be found. Since the aircraft must be as silent and environmentally friendly as possible, the wing loading is limited to $W/S_{DesignPoint} = 500 \text{ kg/m}^2$ due to the reasons above. The aim is to be able to fly as slow as possible during departure and approach, avoiding use of high-lift devices whenever possible. The cruise speed is negatively impacted but the expected fuel consumption is improved. On the other hand, the climb curve limits the permitted design area ($T/W=0.29$). The Thrust-to-Weight ratio is increased to $T/W_{DesignPoint} = 0.3$. A better climb performance assures a relatively greater distance between aircraft and sources at ground level experiencing the flight noise. According to the inverse sound square law, increasing the distance is a very effective way to reduce the noise impact.

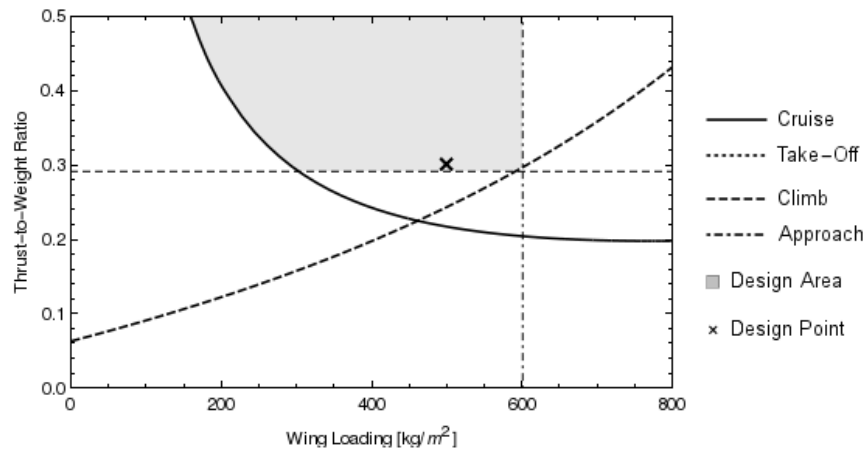


FIG. 4: Thrust-to-Weight Ratio against Wing Loading for designed aircraft *AquisPlane*

IV.2. Engine Design

During Initial Sizing it was approximated that around 236 kN is required for accelerating at take-off conditions. This assumption was confirmed by the engine scaling factors of climb and cruise. For cruise maximum rotational fan speed was selected as 87.5% and for climb 93.0%. The efficiency and calculated weights are based on the references [20] [13] [14]. The estimated weight includes refrigerant cooling for the electrical motor and generator. Cryogenic cooling to use superconducting components was also considered, but this technology requires stored LH_2 on-board. This means an additional system and greatly increased complexity. LH_2 cooling is only worthwhile if the aircraft is also LH_2 powered. It was assumed that 25% of the required power for climbing and backup power for engine malfunctions is stored in lithium ion batteries, and 75% is provided by the turbine. The higher overall efficiency of the hybrid propulsion system leads to a lower fuel burn, which means a decreased fuel weight. This reduced fuel weight should compensate for the additional weight of the hybrid system in comparison with normal turbofan engines. The gaseous emissions are reduced due to the higher efficiency and the loss of power redundancy is improved due to the backup batteries. The four electric fans work like the fan of conventional turbofan engines. They are basically a ducted propeller and were calculated with classic propeller theory. Instead of the gas engine core, an electric motor is driving the fan. Thus, no gaseous pollutant is produced in the fans. The PMAD works as gearbox between the engine-generator-unit and the fans. The rotational speed of the fans is used for controlling thrust, while the turbine rotates at the efficiency optimal rotational speed. The diameter and efficiency of the fans have been estimated based on existing turbofan engines. The Table II provides an overview of the calculated engine design data:

TABLE II: Engine Design Parameters.

Parameter	Value	
Engine Scaling Factor Cruise	0.671	
Engine Scaling Factor Climb	0.946	
Thrust	236 kN	
Fan Diameter	2 m	
-	-	
Component	Efficiency	Weight [kg]
Engine	0.4	1300
Generator	0.997	1000
Motors	0.994	400 each
PMAD	0.9	-
Fan + Nacelle + Pylon	0.9	1000
Lithium Batteries	1000	800
-	-	-

IV.3. MTOW Estimation

Maximum take-off weight was estimated with Eq. 1 using Raymer's iterative approach [15] :

$$MTOW_{Raymer,i} = W_{Crew} + W_{Payload} + \frac{W_{Fuel}}{MTOW} \cdot MTOW_{i-1} + (frac{W_e MTOW)_{i-1} \cdot MTOW_{i-1} \quad (1)$$

where in Eq. 1, W_{Crew} represents the crew weight is composed of 2 pilots and 5 flight attendants. The weight per flight crew member is 85 kg and for cabin crew members is 75 kg [21]. This makes the weight of the crew $W_{Crew} = 545kg$. The payload weight is estimated assuming 210 passengers and cargo mass. A mass of 90.72kg per passenger is used as a reference value [21]. Cargo is assumed to be 15% of the total payload. The resulting payload is therefore $W_{payload} = 22413.2kg$. The fuel fraction is calculated taking into account the required fuel for every mission segment: taxi, climb, cruise, descent, go-around, wait and landing. All these parameters are assumed to be constant and are calculated using the guidelines in [15]. The empty weight fraction was calculated using a semi-empirical formula which takes the Weight, Mach-Number, Thrust-to-Weight, Wing-Loading and aspect ratio as inputs:

$$\frac{W_e}{MTOW_i} = 0.32 + 0.66 \cdot MTOW_i^{-0.13} \cdot A^{0.3} \cdot \left(\frac{T}{MTOW}\right)^{0.06} \cdot \left(\frac{MTOW}{S}\right)^{-0.05} \cdot M_{max}^{0.05} \quad (2)$$

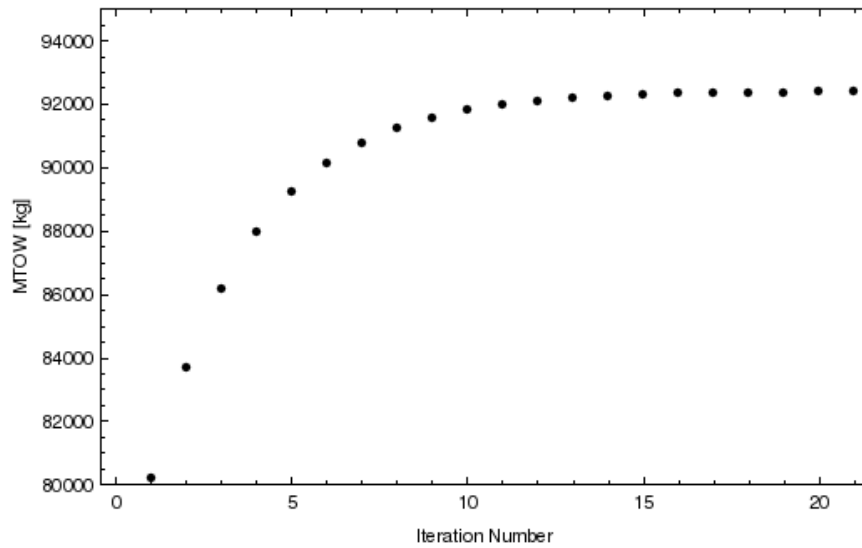


FIG. 5: Iterative calculation of the MTOW

Having been developed in the late 80s based on even older designs, the empirical coefficients used in the empty weight fraction formula are not state of the art any more. A technology coefficient according to (3) is used to get a more realistic MTOW value taking into account technology and design advances.

$$MTOW = MTOW_{Raymer} \cdot K_{tech} \quad (3)$$

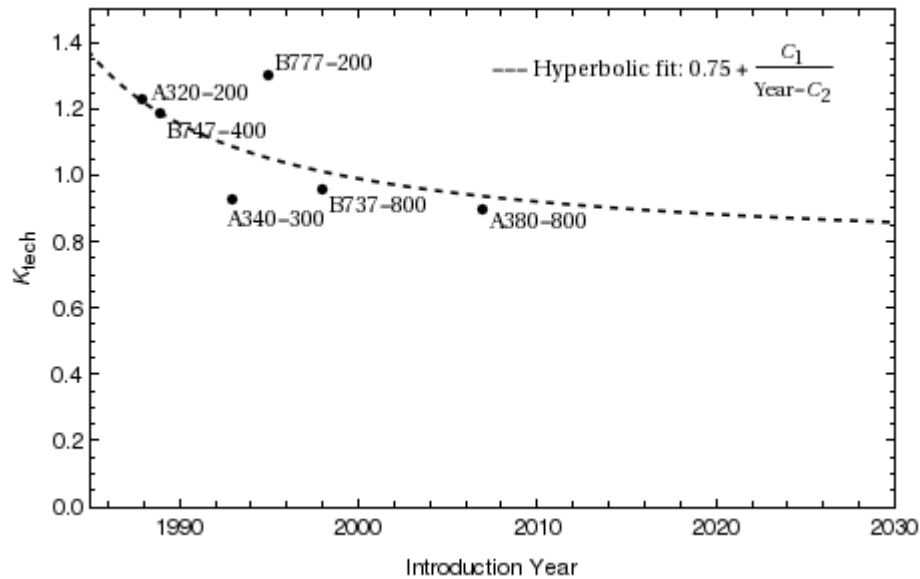


FIG. 6: Technology coefficient regression

In order to determine the technology factor K_{tech} a hyperbolic fit is applied to the calculated values of six known transport aircraft Fig. 6. The fit is constrained to $K_{tech} = 0.75$ at infinity to avoid overly optimistic results. According to the diagram a value of $K_{tech} = 0.85$ can be assumed for an aircraft introduced in 2025-2030. This yields an estimated MTOW of 78540 kg. After calculating the values of the individual systems (wing, gears, propulsion system, etc) this value will have to be revised in chapter IV.8.

IV.4. Fuselage Configuration

The *AquisPlane* is intended to transport up to 210 PAX, with the use of a simple aisle cabin. To optimise the use of space a total row width of 6 seats was selected, 3 either side of the aisle. Regarding the projected growth in air traffic over the next 20 years and increased demand for reasonable pricing at higher volumes whilst still maintaining comfort, it is considered optimal to outfit the standard aircraft with a single, economy, class. To accomplish this the *AquisPlane* is intended to both transport the maximum number of passengers and provide reasonable levels of comfort. This will be achieved by installing two kitchens and four toilets. The number of emergency exits are designed to be 4. The aircraft length is composed of the cabin-, cockpit-, and tail-length, and comprises a total of 53 m. This approximate value was calculated using the Eq. (4) given by Howe [22]:

$$L_{cabin} = ((\frac{PAX}{n_{SA}} + n_{kitchen}) \cdot P_{seat} + n_{toilets} + 0.8 \cdot n_{CrossAiles}) \quad (4)$$

Where P_{seat} is the seat pitch, selected to be 0.81. Cockpit and tail length can both be approximated by Eq. (5) and Eq. (6) [17].

$$l_{Cockpit} = 1.7 \cdot d_{Fuselage} \quad (5)$$

$$l_{Tail} = 3 \cdot d_{Fuselage} \quad (6)$$

Whereas $d_{Fuselage}$ the total diameter is provided by Eq. (7):

$$d_{Fuselage} = 0.5 + n_{sa} + 0.55 \cdot n_{Aisles} + 0.3 \quad (7)$$

The cargo bay volume of the designed aircraft *AquisPlane* has a volume of 282.5 m^3 and an estimated 15% mass fraction of the total payload.

IV.5. Wing and Empennage Design

The main wing is realised as a high wing at the tail of the designed aircraft. This allows for a better lateral stability and an undisturbed air-stream on the topside [23]. On the basis of MTOW and the chosen design point, the parameters were calculated as shown in Table. III below.

TABLE III: Wing Parameters

Parameter	Value
Wing Area (S)	144.9 m^2
Aspect Ratio	10
Wingspan (b)	38.7 m
Swept angle	22.54 degrees
Swept angle LE	25.47 degrees
Swept angle TE	13.01 degrees
Taper ratio	0.24 degrees
Chord of wing root	6.14 m
Chord of wing tip	1.47 m
Wing depth	4.28 m
Span of wing depth	7.57 m
Wing tip symmetric line	46.22 m

The task of compensating out the pitching moment will be conducted by the canard at the front of the designed aircraft. The advantages of this concept are gentle stall characteristics and a better lift distribution which is further improved by the forward swept angle. In contrast to conventional tail units the canard produces positive rather than negative lift. To avoid an unfavourable incident flow of the main wing, the canard is placed at the bottom as a low wing. The vertical stabiliser is positioned under the main wing on both sides at a distance of 8m from the centre-line and contains the landing gear. The vertical stabiliser also functions as the fairing for the gear and therefore reduces the noise impact of the landing gear especially during approach. The calculated and set parameters are shown in Table. IV

TABLE IV: Empennage Parameters

Parameter	HTP	VS
Momentarm	30.84 m	9.28
Stabiliser Area	18.13 m^2	48.2 m^2
Aspect Ratio	10	1.2
Span	13.46 m	7.61 m
Swept Angle	-20.38	25.57
Taper Ratio	0.321	–
Chord of Wing l_{root}	2.05 m	2.212 m
Chord of Wing l_{tip}	0.64 m	–
Reference Chord	1.04 m	–
Span-wise Location of Reference Chord	2.24 m	–
Volume Coefficient	0.9	0.08

IV.6. Control Surfaces and High Lift Devices

After the definition of the general design and wing position the control surface design is determined, using general recommendations for the required areas. With consideration of a relatively large moment arm from the forward horizontal stabiliser to the CG, the elevators can be rather small with a combined span of 10.9 m and an area of 4.1 m^2 . Due to the root and tip design, the elevator extends from 0.1 to 0.9 of the relative half span of the canard wing. The aileron design differs not significantly from a standard design. The combined span is determined to 16 m with an area of 6.4 m^2 , positioned at 0.5 to 0.9 relative half-span of the main wing. The rudder design is more critical, since the moment arm to the CG is relatively small. Therefore, the rudders are expanded to the complete span of the vertical stabilisers with a combined area of 12.8 m^2 . To prevent a rudder strike, the lower edge is shortened and the upper edge slightly enlarged to regain the lost area. In contrary to a standard design of the high lifting devices the selected design profits from the additional lift generated from the canard. The remaining required lift during the

critical phase for high lift devices, the take-off, is generated by standard single-slotted flaps and an adaptive leading edge on the main wing. To achieve the designated $C_{l,max} = 1.93$ the flaps are installed from 0.1 to 0.5 relative wing span with a chord length of 0.3 in relation to the total wing chord and a maximum angle of 30 degrees. The possible d_{Cl} for this flap type is calculated with Eq. 8,

$$C_{la,f} = C_{l,alpha} \cdot [1 + 2 \cdot (z_{hf}/c) \cdot \tan(d_f/2)] \quad (8)$$

For the remaining increase in $C_{l,max}$ the slats are needed. Ordinary slats can increase it for additional 0.4 points, since we are using an adaptive leading edge, we have to expect a decrease in $C_{l,max}$ of up to 0.2 points. Regardless the needed lift coefficient can be achieved.

IV.7. Landing Gear Design

The selected landing gear configuration is the commonly used tricycle configuration, here with the main landing gear integrated into the vertical stabiliser. A maximum track width of 16 m allows for the greatest possible lateral stability on the ground and supports the weight of the wing on the ground. The nose landing gear is longitudinally positioned directly behind the gas turbine, in the space between the outlets. The position of the main landing gear is determined by the location of the vertical stabiliser at $x_{Fm} = 52.18 \text{ m}$. The structural length of the gears was defined as $L_{Gear} = H + S_{LG,compressed}$. The distance between the fuselage and the ground was set as $H : 0.6 \text{ m}$ and the compressed suspension of the landing gear $S_{LG} : 0.3 \text{ m}$ which gives a gear structural length $L_{Gear} = 0.9 \text{ m}$. Verification of the rear-angle -clearance requires the tilt angle Y to be greater than 10° . Because of the main gear at the back the tilt angle Y of the designed aircraft is 19.88° . For the wing-tip clearance, an angle of 5° should be the minimum. The high-wing configuration and over-wing engine mounting provide an advantageous angle of 14.82° . For the calculated maximum take-off weight, 4 wheels and 2 legs are recommended for the main landing gear, as one wheel carries a load of about 30,000kg [24]. The main landing gear will consist of 6 wheels, 3 each side, to reduce the specific loading and allow a reduction in the wheel dimensions. The wheels are to be longitudinally aligned reducing the required width of the vertical stabilisers. The wheel track of 16 m is more than twice as much as the wheel track of an Airbus A320-NEO (7.59 m). This, along with the low-lying fuselage, generates an enormous benefit in lateral stability. At 0.6 m the fuselage is 1.12 m closer to the ground than the comparison vehicle, the A320-NEO (1.72 m) [9] resulting in an additional reduction in the structural weight of the landing gear struts. The shorter struts lead to a drag and therefore noise reduction. Since the gear supports the wing on the ground, the structural weight of the wing can also be reduced. By integrating the main landing gear into the vertical stabiliser, the necessity for heavy and complex retraction machinery is eliminated. Instead a simple aerodynamic fairing will enclose the main gear during flight. An overview of the parameters is presented in Table. V.

TABLE V: Tri-cycle Landing Gear Parameters for the designed aircraft.

Parameter	Value
Wheelbase	47.02 m
Wheel track	16 m
Distance b/w Fuselage & Ground	0.6 m
Structural Length	0.9 m

IV.8. Component Mass Estimation and Center of Gravity

In the preliminary design of a new civil aircraft the estimation of component masses is of high relevance. It is not only important that the aircraft be as light weight as possible for economic reasons, but the mass of the different parts has to be known for certain design parameters (centre of gravity, wing position etc.). Here, maximum take-off weight (MTOW), mass of the fuselage, wing, horizontal and vertical stabiliser, propulsion, avionic systems, pylons, operational items, fuel and fixed cabin equipment is estimated. The maximum take-off weight was iteratively estimated in chapter 4. It will be used for the following calculations here. The mass of the fuselage is defined here as only the structural weight and was estimated using Eq.(9) according to [22].

$$M_{Fuselage} = K_{Howe} \cdot [1 + (3.12 - 0.354 \cdot d_{fuselage}) \cdot \frac{2s}{1+s}] \cdot [3.56 \cdot \frac{P_{max}}{s^{0.75}} \cdot S_{wetted,fuselage} \cdot d_{fuselage}] \quad (9)$$

Where the correction factor K_{Howe} is 1 for aircraft with landing gears integrated in the wing. \bar{s} takes into consideration the tensile tensions in the fuselage and is calculated to 0.385 with the fuselage diameter $d_{fslg} = 3.85$. The pressure P_{max} [bar] is the maximum difference between cabin and outside. The pressure in the cabin is equivalent to a height of 2400 m and the minimal environmental pressure is at a height of 11700 m for a mid range aircraft. These pressure values were calculated according to ISA values. $S_{wetted,fslg}$ is the wetted fuselage surface area. The mass of the wing was estimated using the Eq.(10) below according to Schöffel and Sanders [25] and comprises the structural weight of the wing box, the control surfaces, fairings and winglets. Systems such as the actuator and fuel distributors along the wing were not taken into consideration.

$$M_{Wing} = 0.018 \cdot (MTOW)^{1.39} \cdot L^{1.04} \cdot \left(\frac{MTOW}{S_{Wing}}\right)^{-0.695} \cdot n_B^{0.695} \cdot \left(1.1 + \frac{l}{2}\right)^{0.695} \cdot (f_E)^{0.695} \cdot (f_g)^{1.0425} \cdot (f_d)^{-0.695} \cdot \cos^{-1.0425}(f_{25}) \quad (10)$$

Here, L , l , S_{Wing} are defined as the wing design parameters, while $n_B = 3.75$ is the failure load factor. The engine factor is $f_E = 0.85$ for four engines on the wing. Where the constant $f_q = 1.14$ considering ram pressure. The influence of the thickness of the wing at root is defined as $f_{d/c} = 13.28$.

The mass of the canard and the vertical stabiliser plane, along with their control surface was estimated using the Eq. (11) and Eq. (12) according to [22] as following:

$$m_{HTP} = 0.047 \cdot V_D \cdot (S_{HTP})^{1.24} \quad (11)$$

Where the drive velocity is $V_D = 220$ m/s and the surface of the canard is S_{HTP}

$$m_{VS} = k_1 \cdot 0.065 \cdot V_D \cdot (S_{VS})^{1.15} \quad (12)$$

Here k_1 is a factor for considering T-tail planes it is equal 1 for conventional tail planes and S_{VS} is the surface of the vertical stabiliser plane respectively. The mass of the landing gear is determined as a group mass with a scaled function of Torenbeek [26]. It is then split into nose gear factor

$$m_{LG} = 0.00271 \cdot MLW^{1.24}$$

and main landing gear with factor

$$M_{\frac{NG}{M}} = X_{\frac{NG}{MG}} \cdot m_{LG}$$

. Here, maximum landing weight (MLW) is estimated as 64500 kg as on an Airbus A320, and the factors $X_{NG} = 0.15$ and $X_{MG} = 0.85$ for a middle range aircraft. The mass of pylons was calculated with the Sea Level Static Thrust (SLST) using the Eq. (13)

$$m_{Pylon} = 0.0024 \cdot SLST + 233.29 \quad (13)$$

The mass of the propulsion system is estimated regarding the most power demanding period in the mission profile, the go-around. Using the Thrust-to-Weight ratio and MTOW the total thrust is calculated. Multiplied with the velocity in a go around case and divided by an efficiency factor of 0.89 for our electric propulsion system, the needed shaft power is derived. According to [20], the weight weight of an appropriate gas turbine can be determined. Assuming 2000 kg per engine (1000kg each E-Fan and motor) the mass of the nacelle is calculated.

With four engines the total mass is:

$$m_{Propulsion} = (m_{Engine} + m_{Nacelle} + m_{EngineSystems}) \cdot 4$$

The mass of the systems was determined as a group mass assuming a $MTOW < 225000$ kg with the following regression:

$$m_{Systems} = 1.781 \cdot 10^{-7} \cdot MTOW^2 + 8.07 \cdot 10^{-2} \cdot MTOW$$

The mass of fixed cabin equipment is dependent on the number of passengers. Flight deck, crew seats, water system, floor covering, fire protection, escape equipment, oxygen, cargo and miscellaneous equipment were estimated according to [17] and grouped together as fixed cabin mass. The mass fuel mass was roughly estimated with MTOW using the Eq.(14). This is because at this moment in design the exact fuel consumption is not known.

$$m_{Fuel} = MTOW - OEW - m_{Payload} \quad (14)$$

Building the sum of these masses the so called Manufacturers Empty Weight (MEW) is derived. To consider lightweight materials and better production techniques in the future MEW is multiplied with the technology factor $K_{tech} = 0.85$. The mass of operational items includes the crew with their baggage, food storage, life jackets etc. and can be determined for short and middle range plane using the Eq.(15) from [22]:

$$m_{opItems} = 85 \cdot N_{crew} + 12 \cdot PAX \quad (15)$$

A weight build up summary is provided in Table. VI below.

TABLE VI: A summary of the weight buildup of the designed *AquisPlane* aircraft.

Parameter	Value [kg]
Fuselage	11616
Wing	9414
Canard	376
vertical stabiliser Plane	1233
Nose Gear	351
Main Gear	1988
Pylon	788
Structured Weight	25766
Propulsion	10858
Systems	5240
Cabin Equipment	4769
MEW	46633
$K_{Tech} \cdot \mathbf{MEW}$	39638
Operating Equipment	3030
OEW	42668
Fuel	17279
Payload	22413
MTOW	82360

The final centre of gravity of the aircraft is calculated with a momentum equilibrium to the sum of the centre of gravity of the different components as

$$X_{CG,a/c} = \frac{(\sum m_i \cdot X_{CG,i})}{\sum m_i}$$

The moment arms of the components are referring to the nose and are calculated by a few simple assumptions yielding from the aircraft geometry. To ensure flight stability the total centre of gravity has to be between the foremost and rearmost limits in all situations. These limits are determined from different loading scenarios shown in the Table. VII.

TABLE VII: Payload Range Configurations

Payload Range Combination	$x_{CG,a/c}$ [m]	$x_{CG,a/c/l}$ [-]
MEW	41.7	9.7
No Payload & Fuel	40.4	9.4
Max Payload & No Fuel	36.7	8.9
Max Payload & Fuel Till MTOW	40	9.3
No Payload & Max Fuel	44.1	10.3
Foremost CG Position	36.8	8.6
Rearmost CG Position	44.2	10.3

IV.9. Stability and Control

Flight stability and control design are key elements in aircraft design, especially for aircraft flying at high speeds. According to [15], aircraft with similar tail volume coefficients have similar flight characteristics in both controllability and stability. The statistical data available for transport jets [16, Table 8.7] are however limited to classic configuration aircraft. This method will suffice, however, as a first approach for the dimensioning of the stabilising surfaces. Eq. (16) and Eq. (17) show the definition of the volume coefficients for the vertical (VS) and horizontal (HS) stabilisers.

$$c_{VT} = \frac{L_{VT} \cdot S_{VT}}{b_W \cdot S_W} \quad (16)$$

$$c_{HT} = \frac{L_{HT} \cdot S_{HT}}{b_W \cdot S_W} \quad (17)$$

Longitudinally unstable aircraft are highly manoeuvrable and often more fuel efficient. The more unstable the aircraft, the more complex its flight control system will be. To keep the complexity of an already very innovative design low, *AquisPlane* is designed to be longitudinally stable at every CG position instead of having relaxed stability. This way, in the case of a flight control system failure the pilot should be able to fly and land the aircraft safely with a mechanical backup. For this, a conservative tail volume coefficient $c_{HT} = 0.9$ was chosen. For the lateral stability a fin volume coefficient of 0.05 was used. While in the lower range of known values according to, there are other jet transport aircraft like the BAC 1011 ($v_{VT} = 0.038$) with lower values.

This calculations should only be seen as a first estimation to achieve a stable and controllable aircraft. A full control analysis will be needed to ensure that the aerodynamic surface parameters are correctly sized, especially for landings with a forward CG position.

V. ENVIRONMENTAL

Since the reduction of noise emission is one of the central aspects of the designated design, it has been a major focus of our work. The past noise reductions for current aircraft have mainly resulted out of small improvements such as Chevron nozzles or geared turbofans. To meet the goals of the vision for 2050 these small improvements can contribute, but are not able to achieve the reduction that is needed. During our design, we focused on three main noise contributors: fan noise, jet noise and airframe noise for a significant overall reduction. These three represent the most important noise sources of current aircraft, with differing contributions to the total noise emissions depending on the flight stage.

V.1. Jet Noise

Jet noise is the part of the engine noise emitted by the accelerated outlet of the engines, and a main contributor to the take-off noise emissions. It is generated by the shearing stress between the accelerated engine stream and the surrounding steady air stream. These tensions lead to pressure fluctuations and finally to a typical broadband noise. For a possible reduction, the hotter and faster inner stream of today's engines is of significant interest, since

the acoustic power of a subsonic stream has a dependency of v^8 . A reduction in overall stream velocity leads to a reduction of acoustic power with v_s^8 , demonstrating the advantage of a high-bypass-ratio engine with a much lower speed in the outer stream. For a further jet noise reduction, we chose to use electric engines, eliminating the combustor and turbine noise and the hot inner stream as a noise source. Also, since four instead of two engines are used, the resulting thrust of the single engines will be much lower than the one of an engine of a comparable aircraft and the outlet speed will be even slower, leading to a further decrease in noise output. For a first estimation we compare our design to an A320 with two V2527-A5 engines. For the fan outlet we are assuming the density of the outer stream, half the acceleration and an outlet area of 2 m^2 . With these first estimations we obtain a possible reduction of 19 dB. Due to the unknown frequency distribution this Sound Pressure Level (SPL) cannot be weighted according to the A-filter or converted into EPNdB, but it can be assumed, that by the enlarged outlet area the peak frequency will be moved towards lower frequencies leading to a lower dB(A) level and Effective Perceived Noise Level (EPNL). The design is completed by Chevron nozzles at the engines. This nozzle geometry prevents a sudden mixing of the accelerated and un-accelerated streams, resulting in a better mixing with less stress. Additionally, implementation reduces low-frequency noise with a possible increase at higher frequencies. Since the peak frequency is decreasing the increase in higher frequencies is accepted, achieving a SPL reduction of up to 8 dB at 1 kHz [27]. Overall estimates suggest a total jet noise reduction of about 26 dB.

V.2. Fan Noise

Fan noise is the main noise contributor in the sound field in front of the aircraft. It is influenced by the rotation speed of the blades and the tip Mach number resulting in a broadband noise with significant tones at the fan blades fundamental frequency and their higher harmonics. These tones, resulting in the typical fan whine, have a high influence on the actual annoyance of aircraft noise. In the early stages of the engine concept it was decided that shielding is the best and easiest way to approach the problem of fan noise reduction. As a result the engines are mounted on top of the main wing rather than slung below, achieving a forward shielding angle of 60° for the outer engines and 40° for the inner engines. This shielding will have a noticeable impact on fan noise contribution below these angles, however the actual reduction cannot be calculated here.

A further reduction results out of the acceleration reduction in the engine stream, leading to a lower rotation speed and blade tip Mach numbers.

V.3. Airframe Noise

In contrary to the other two noise sources the airframe noise can occur in different variations. The major sources we considered in our design are landing gear and high-lift devices as the two main contributors to total airframe noise [28]. The landing gear is a main noise source during the approach with broadband as well as tonal noise, which can be of relevant annoyance. To reduce this noise source we focused on covering as much as possible of the gear, with a maximum noise reduction of about 10 dB [28]. As promising as the resulting noise reduction seems, the additional weight has to be considered. To eliminate this problem, we decided to install the landing gear inside of the vertical stabilisers, acting as a cover for the most part of the suspension and gear leg. However, due to tail strike and suspension criteria, a complete cover cannot be achieved. The gear suspension and main systems are integrated into the vertical stabilisers; what remains in the free stream outside are the wheels and a short part of the gear leg for a significantly reduced gear noise. To integrate the gear the layout is changed to three wheels in a row rather than the classical double tires. In addition, the smaller wheels are beneficial for the generated noise since the acoustic power of the wheels has a dependency of d_{wheel}^2 [29].

The noise of flaps and slats is generated by the gaps, specifically the resulting vortex between the wing and the device. For the further considerations, we focus on the approach where the high lift devices are fully expanded. During the approach the flap noise is considerably lower than the slat noise [30] and is therefore not further dealt with. Now to reduce the slat noise the inner vortex has to be reduced or prevented. Reductions can be achieved by flexible transitions on the lower part, however a complete prevention of noise is not possible in this manner. This thought allowed to make use of geometrically optimised adaptive leading edges from composite materials in the designed aircraft. There exists a plethora of designs for leading edge adaptive systems and in this designed a morphing leading edge with high lift position and integrated actuators was envisioned. This allows to circumvent the generation of vortices. This method entails a slightly reduced c_l , but the decrease is small enough not to affect the required aerodynamic performance. After these changes and the elimination of slat noise and a gear noise reduction of minimum 10 dB, the dominant noise source will be the remaining flap noise. Since this source is not changed in

our design, it will remain on its level at about 6 EPNdB below the slat noise [30], which means an effective reduction in airframe noise of these 6 EPNdB.

Altogether, a massive reduction in jet noise and a significant reduction in airframe noise was achieved. The shielding effect of the main wing will also have a significant effect on noise reduction. After implementing all the presented changes, other noise sources than the engine will likely become predominant at a lower OASPL. However, during this design process no exact analysis of the noise emissions after the implementation was possible and a second reduction iteration was waived.

VI. COSTS

The costs for developing and producing an aircraft are usually differentiated between Recurring (RC) and Non-Recurring Costs (NRC). RC are due to use of materials, payment of workers, electricity and such during production. The costs for all the Engineering services (RD, tools, professionals) and investments in assembly lines for producing the aircraft are placed under NRC. A non-conventional aircraft like the *AquisPlane* will need more NRC than the currently flying models of known companies. However, it is still in the dimensions of a comparable aircraft (A320) which benefits from the available infrastructure in production. The biggest part will be developing and testing the new propulsion system and getting all the certifications needed for operational flight. With new business models and economies of scale, the RC wont be significantly higher than current aircrafts for the *AquisPlane* once it enters service. There could even be potential savings by the reduction in the use of expensive kerosene turbines, after the simpler E-Fans are developed. Designing an all new Aircraft is mostly driven by the operating costs, divided in direct (DOC) and indirect operating costs (IOC). While the IOC will be roughly the same as for an A320, there is big saving potential in DOC as the fees paid to the airport for an aircraft are dependent of its emissions, which will be reduced to a minimum with *AquisPlane*. The expensive maintenance of two or more aircraft engines will be replaced by one simple gas turbine. Additionally, the airlines will benefit from the more efficient propulsion system using less fuel.

VII. CONCLUSION

The design approach was based on an analytical investigation of current technologies and construction methods, rather than an attempt to reach into non-realised systems and technologies, to ensure the projected 2025-2035 delivery time frame. The final aircraft design relies upon technologies at or near industry maturity, albeit in adjusted configuration to improve on the critical design points. The *AquisPlane* is developed around improvement of exhaust emissions and noise pollution. The design is deliberately conceptually innovative in an attempt to break standard aircraft paradigms. The *AquisPlane* shares much in common with a conventional airliner: quasi-cylindrical fuselage with a main wing to produce lift, row-arranged seating, external propulsion systems, and a system of stabilising flight surfaces. However here the similarities end.

The propulsion system is a hybrid fuel-electric powered system, with a single internal gas turbine engine providing power to four external electric ducted fan thrusters with a maximum thrust of 236 kN. The generator also provides internal system power and charges a battery bank in low-thrust flight regions for backup power. The decoupling of the thrust and power generation systems allows multiple efficiency improvements. The increased efficiency of the hybrid system reduces overall exhaust emissions, as well as providing flexibility in fuel usage during flight. One primary advantage is the ability to land with the main turbine switched off, greatly reducing noise and exhaust pollution in the airport vicinity. Physically, the *AquisPlane* is a canard-configuration aircraft. The main wing is mounted to the rear, in high-wing configuration. The high wing improves lateral stability and provides additional protection to the electric fans mounted above it. The twin vertical stabiliser and integrated main landing gear are situated below the main wing on either side, delivering advantages in structural requirements and noise emissions, particularly during take-off and landing. The reduced moment arm of the vertical stabiliser in relation to the centre of gravity is accounted for by the increased wetted area of twin surfaces. The forward swept canard wing provides improved lift distribution, gentle stall characteristics and above all others, eliminates the need for a negative lifting surface at the tail of the aircraft. The switch from a negative-lift horizontal stabiliser to a positive-lift canard wing delivers a significant improvement to the flight characteristics and overall cruising efficiency of the *AquisPlane*. The modified tricycle landing gear configuration offers multiple advantages. The wide-spaced main landing gear under each wing provides significant lateral stability to the aircraft in taxi, landing and take-off conditions. The low ground clearance (0.6m) reduces the required structural weight as well as significantly improving the aerodynamic and noise emission characteristics over a conventional design whilst deployed. The under-wing landing gear also reduces the structural requirements for the main wing.

Overall, through configurational changes utilising currently or soon-to-be available technologies, the *AquisPlane* achieves improvements in multiple areas over currently flying standard-configuration airliners. Rearrangement of the wings and flying surfaces improves the handling and flight efficiency, whilst altered landing gear provide multiple small-scale benefits, particularly regarding the high-value noise emissions on landing and take-off. The largest improvement and centrepiece is the adoption of a hybrid gas-turbine/electric fan thruster configuration, which truly revolutionizes the functionality and efficiency available to the commercial airliner. Greatly improved fuel efficiency, reduced flight emissions, and last but not least, the ability to land and taxi turbine-out.

-
- [1] S. Bruner, *N+3 Phase I Final Review*, Tech. Rep. (Northrop Grumman Corporation, 2010).
 - [2] MIT, Aurora Flight Sciences, and Pratt & Whitney, *NASA N+3 Report*, Tech. Rep. (NASA Langley Research Center, 2010).
 - [3] R. H. Liebeck and T. Hynes, *Journal of Aircraft* **41**, 10 (2004).
 - [4] A. Diedrich, J. Hileman, D. Tan, K. Willcox, and Z. Spakovszky, in *44th AIAA Aerospace Sciences Meeting and Exhibit* (American Institute of Aeronautics and Astronautics, Reston, Virginia, 2006).
 - [5] E. de la Rosa Blanco, C. Hall, and D. Crichton, in *45th AIAA Aerospace Sciences Meeting and Exhibit* (American Institute of Aeronautics and Astronautics, Reston, Virginia, 2007).
 - [6] General Electric, Cessna, and Georgia Tech, *N+3 Small Commercial Efficient & Quite Air Transportation for Year 2030-2035*, Tech. Rep. (GE Aviation, 2010).
 - [7] M. Bradley, C. Droney, D. Paisley, B. Roth, S. Gowda, and M. Kirby, *NASA N+3 Subsonic Ultra Green Aircraft Research SUGAR Final Review (Boeing Research and Technology)*, Tech. Rep. (Boeing Research and Development, 2010).
 - [8] L. Bertsch, *Noise Prediction within Conceptual Aircraft Design*, Ph.D. thesis (2013).
 - [9] Airbus, *AIRCRAFT CHARACTERISTICS AIRPORT AND MAINTENANCE PLANNING*, Tech. Rep. (Airbus Technical Data Support and Services, 2017).
 - [10] Airbus, *Global Market Forecast 2015-2034*, Tech. Rep. (Airbus, 2015).
 - [11] Boeing, *Current Market Outlook 2016-2035*, Tech. Rep. (Boeing, 2016).
 - [12] Heathrow, *Flight Performance Annual Report*, Tech. Rep. (Heathrow Annual Report, 2015).
 - [13] A. Seitz, O. Schmitz, A. T. Isikveren, and M. Hornung, *Deutscher Luft- und Raumfahrtkongress 2012*, 1 (2012).
 - [14] H. Kuhn, A. Seitz, L. Lorenz, A. T. Isikveren, A. Sizmann, and B. Luftfahrt, (2012), 10.13140/RG.2.1.4833.4889.
 - [15] D. Raymer, *Aircraft Design: A Conceptual Approach, Fifth Edition* (American Institute of Aeronautics and Astronautics, Inc., Washington, DC, 2012).
 - [16] J. Roskam, *Airplane design* (DARcorporation, 1986).
 - [17] E. Torenbeek, *Synthesis of subsonic airplane design* (Springer Science & Business Media, 2013) p. 598.
 - [18] Y. Dobrev, *Initial Sizing von Airlinern mit Jet- oder Turbopropellerantrieb*, Ph.D. thesis (2008).
 - [19] European Aviation Safety Agency, *European Aviation Safety Agency*, 617 (2007).
 - [20] H. D. Kim, G. V. Brown, and J. L. Felder, .
 - [21] EASA, *Annexes to the draft Commission Regulation on 'Air Operations -OPS'*, Tech. Rep.
 - [22] D. Howe, *Professional Engineering* (2000) p. 448.
 - [23] R. Brockhaus, W. Alles, and R. Luckner, *Flugregelung* (Springer Berlin Heidelberg, Berlin, Heidelberg, 2011).
 - [24] G. Roloff, *Aircraft Landing Gear - The Evolution of a System*, Tech. Rep. (Airbus, 2002).
 - [25] RWTH Aachen University, "Themenmodul Flugzeugbau II," .
 - [26] E. Torenbeek, *Synthesis of Subsonic Airplane Design* (Springer Netherlands, Dordrecht, 1982).
 - [27] Civil Aviation Authority, "Measuring and modelling noise — UK Civil Aviation Authority," (2017).
 - [28] W. Dobrzynski, *Journal of Aircraft* **47**, 353 (2010).
 - [29] C. Burley, T. Brooks, W. Humphreys Jr., and J. Rawls, in *13th AIAA/CEAS Aeroacoustics Conference Paper 2007-3459* (2007) pp. 1–19.
 - [30] M. Pott-Pollenske, J. Wild, M. Herr, J. W. Delfs, A. Rudenko, and A. Büscher, *Aircraft Noise Reduction by Flow Control and Active/Adaptive Techniques* (2014).

ACKNOWLEDGMENTS

This report has been prepared voluntarily by a group of interdisciplinary and international students at the Faculty of Mechanical Engineering of the RWTH Aachen University in Germany for a joint competition by German Aerospace Center (DLR) and National Aeronautics and Space Administration (NASA). The goal presented was to design a revolutionary quiet and low Emission Aircraft to reduce greenhouse gas emissions and environmental pollution. We would like to thank **Prof. Rolf Henke** and **Dr. Jaiwon Shen** for providing us the platform to showcase our results. We acknowledge the organizational support from **Dr. Olaf Brodersen**, **Dr. Klausdieter Pahlke**, **Kai Wicke** and **Erwin Moerland**. We are thankful for the incredible support of our advisor **Miguel Yael Pereda** who attended our

design reviews and provided us with valuable feedback. This design work was conducted by ourselves and none of us received funds nor consulted with any industry professionals working in this challenge area. **CC BY-ND 3.0 DE**

VIII. TECHNICAL DRAWINGS

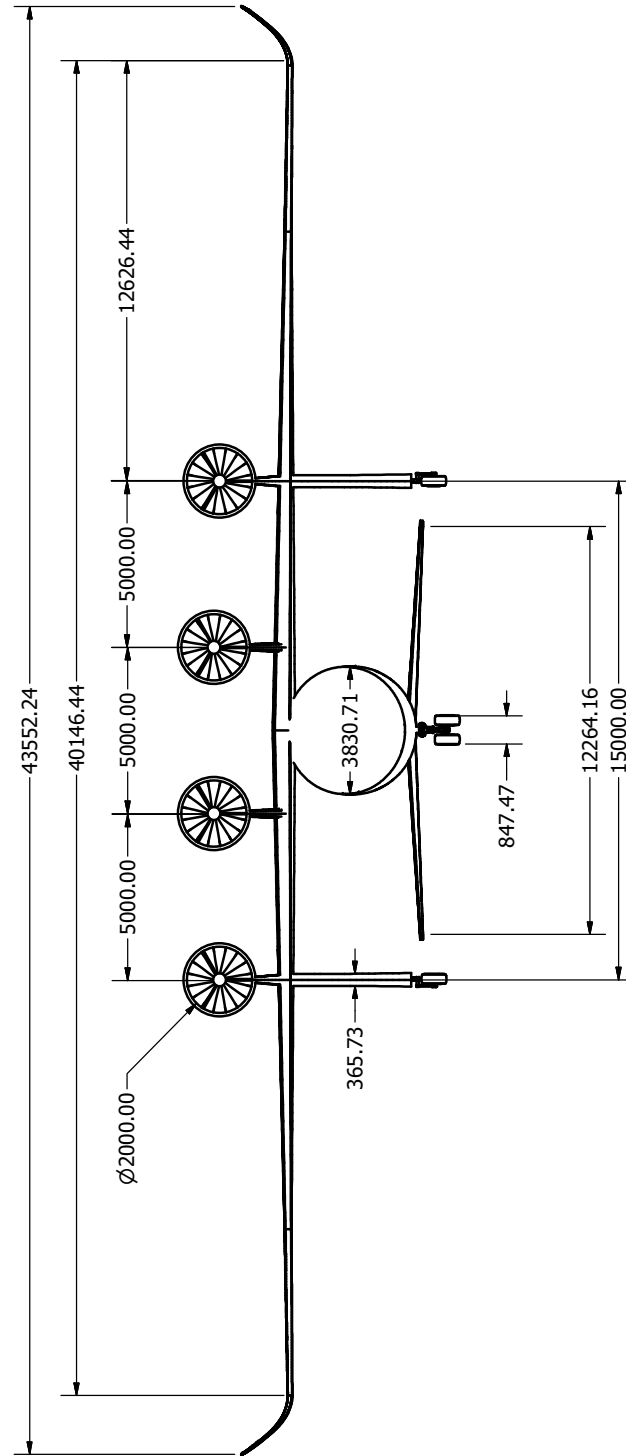


FIG. 7: *AquisPlane* Front View.

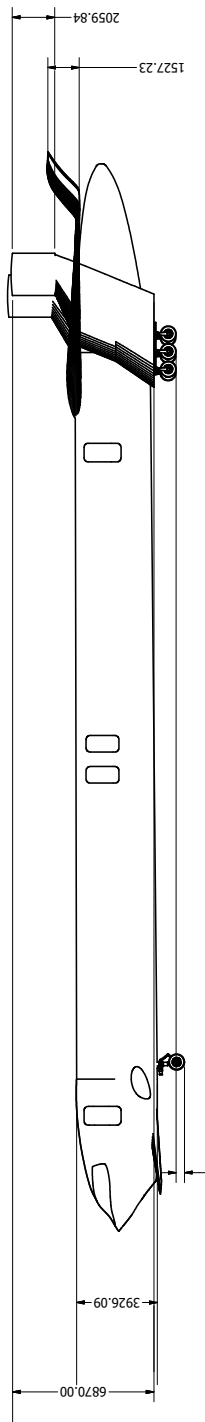


FIG. 8: *AquisPlane* Side View.

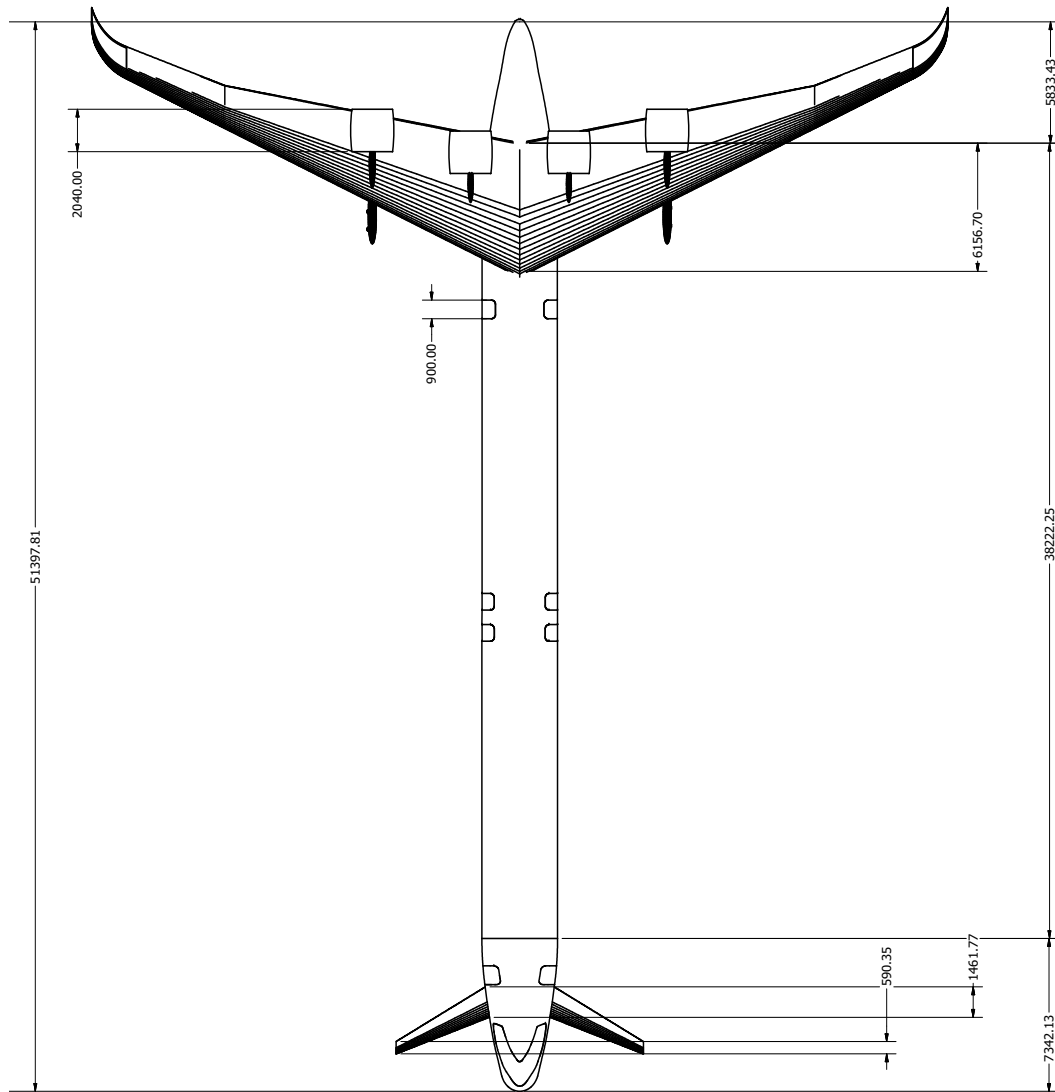


FIG. 9: *AquisPlane* Top View.

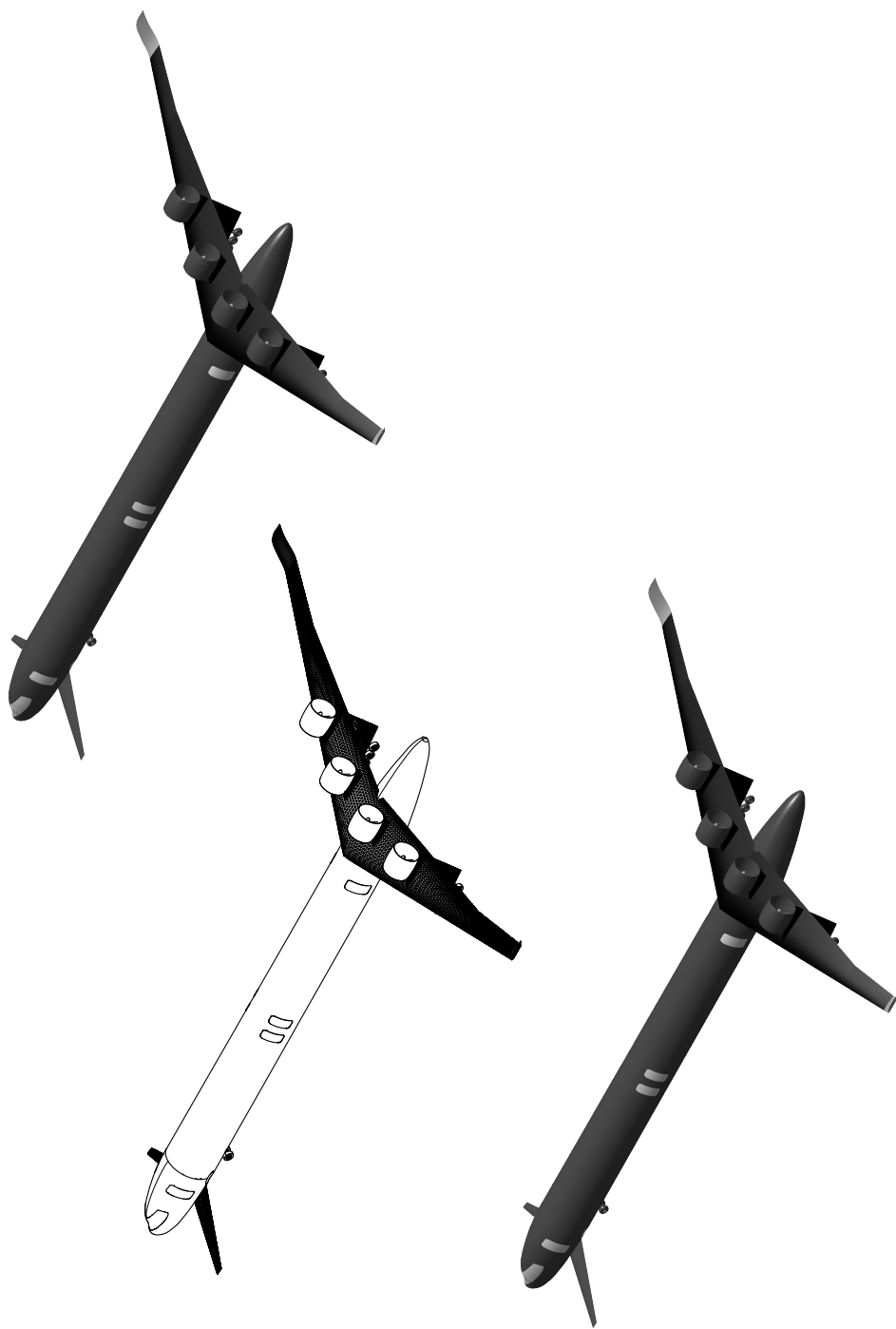


FIG. 10: *AquisPlane* Orthogonic Projection.

AquisPlane

RWTH Aachen University

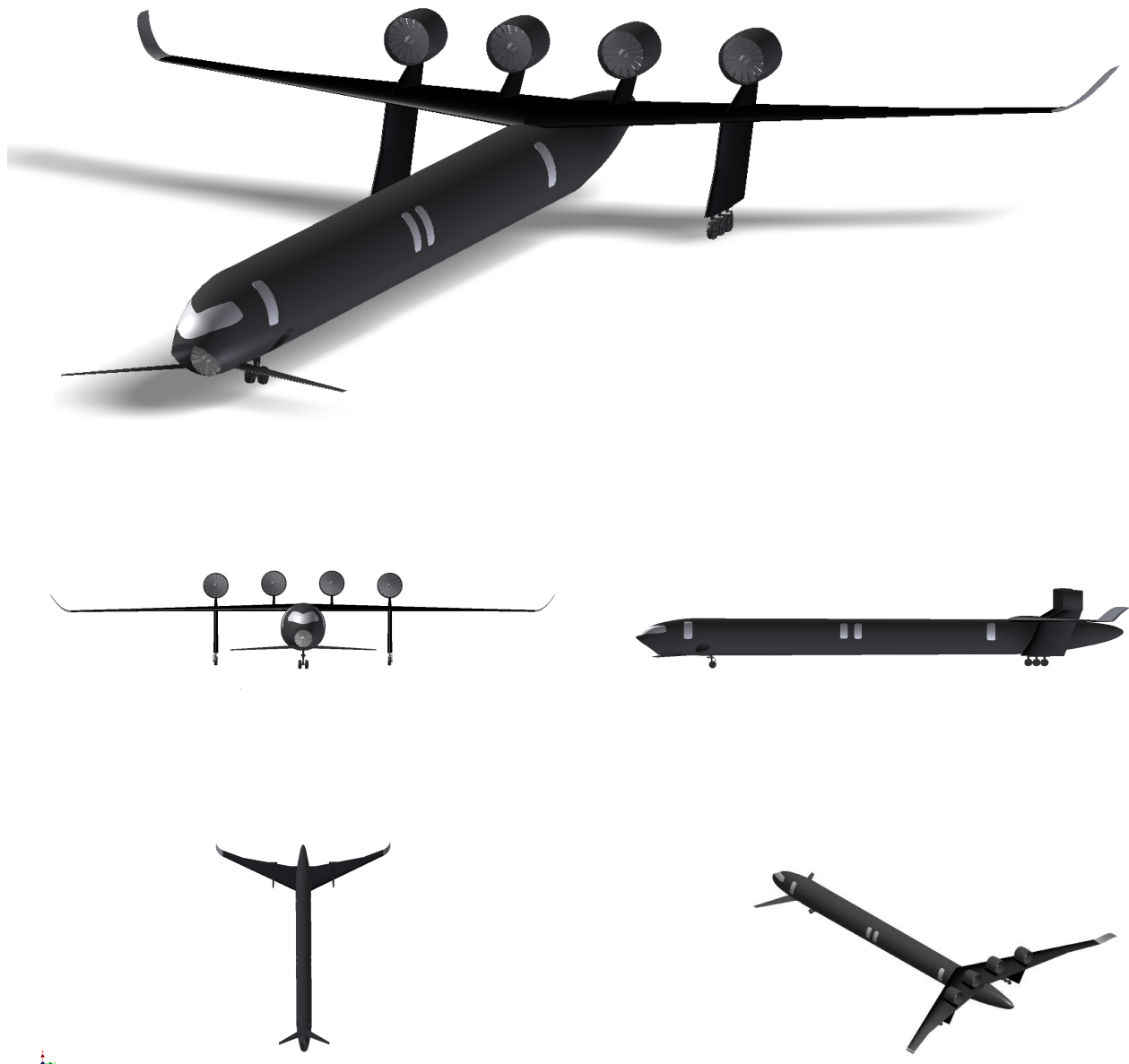


FIG. 11: *AquisPlane* Overview.